

CdS-nanoparticle light-emitting diode on Si

Ching-Fuh Lin^{a*}, Eih-Zhe Liang^a, Sheng-Ming Shih^b, Wei-Fang Su^b

^aInstitute of Electro-Optical Engineering, National Taiwan University, Taipei, Taiwan, ROC

^bInstitute of Materials Science and Engineering, NTU, Taipei, Taiwan, ROC.

*also with Institute of Electronics Engineering and Department of Electrical Engineering

ABSTRACT

The fabrication of CdS-nanoparticle light emitting diodes (LEDs) on Si and their properties at room temperature and variant temperatures are reported. Due to passivation of p-hydroxyl thiophenol group around nanoparticles, 86-meV spectral shift of free exciton transition at room temperature is observed. Controlled conditions for the preparation of CdS-nanoparticle LED such as heat treatment and/or with oxygen-rich environment are found to have significant influences on emission spectra. Radiative recombination of carriers trapped in oxygen-impurity level of 273 meV presents in samples prepared in oxygen-rich environment. Coalescence of nanoparticles into bulk form also occurs to contribute to increased magnitude of luminescence. Spectral behaviors of electroluminescence with varied temperature are studied.

Keywords: Nanoparticle, low-dimensional structures, CdS light emitting diode, temperature effect, Electroluminescence, impurity states

1. INTRODUCTION

Low-dimensional structures like nanoparticles or quantum dots (QDs) are intensively studied recently for their versatile applications in many areas. For light emission purposes, they are supposed to provide significant enhancement in the density of states, so increasing the probability of light emission. There are usually two ways to form those low-dimensional structures. One is the epitaxial technique to grow QDs. The other is using chemical methods to fabricate nanoparticles. The former way is very selective on the grown substrates. Also, QDs are usually formed with only a scarce area density. In contrast, nanoparticles formed by chemical methods have the following advantages. First, they can be applied on any substrates. Second, area or volume density can be very high. The process to fabricate monodisperse nanoparticles is inexpensive and facile to industrial application.

Recently, stimulated emission and optical gain had been demonstrated in CdS quantum dots by methods of optical pumping^{1,2}. This encourages the employment of electrical pumping to realize efficient nanoparticle-based light emitting devices.

In this work, we demonstrate the fabrication of CdS-nanoparticle light emitting diodes (LEDs) on silicon substrate. The fabrication of light emitting active layer is simply the spin-coating technique. Electroluminescence (EL) can be easily achieved by quantum tunneling of carriers into the nanoparticles. The easy EL on Si wafers shows a promising way to monolithically integrate functions provided by nanoparticles and conventional integrated circuitry based on Si. Moreover, light emitting part of opto-electronic integrated circuits can be made after traditional process of electronic part.

The experiments include study of nanoparticle EL behavior in different environment. Heat treatment and mixture of solution is used. Spectroscopy of CdS nanoparticles is significantly influenced by the process temperature and the surrounding oxide. Radiative recombination due to free exciton in CdS is confirmed in these experiments, with pronounced energy shift due to organic coating of nanoparticles. As additional treatment is applied, radiative recombination of oxygen impurity emerges, and coalescence of CdS nanoparticle into bulk form present.

Because the nanoparticles are small (~ 5 nm), compared with bulk materials, a larger surface contact area with environment results. The total amount of impurity states formed by diffusion of oxygen or other contaminants is thus

⁺ Email: cflin@cc.ee.ntu.edu.tw

quite severe and passivation, in our case organic p-hydroxyl thiophenol group, proves to be important. Moreover, the large interface area causes the light emission due to the impurity states to be significant, demonstrating another use of nanoparticles in addition to intrinsic quantum states provided by the low-dimensional structures.

At different temperature, the EL spectrum of CdS nanoparticle remains quite the same. Peak shift is compared with bulk bandgap shift and ascribed as effect of quantum confinement and surface configuration.

2. PREPARATION OF MATERIALS

Redispersible nanoparticle of CdS ready for spin-coating purpose is synthesized by modification of Pietro's method³. Cadmium acetate dihydrate ($\text{Cd}(\text{CH}_3\text{COO})_2 \cdot 2\text{H}_2\text{O}$, 0.80 g, 3.0 mmole) is dissolved in 20 ml mixed solvent of acetonitrile, methanol, and water with volume ratio 1:1:2. Another solution containing disodium sulfide nanohydrate ($\text{Na}_2\text{S} \cdot 9\text{H}_2\text{O}$, 0.36 g, 1.5 mmole) and p-hydroxyl thiophenol (0.56 g, 4.4 mmole) in the same solvent system is added into vigorously stirred cadmium acetate solution. The whole system was stirred for 18 hours without light illumination. After removing solvent and purifying by centrifuge, we obtained 0.70 g yellow solid aggregate of CdS nanoparticles capped by p-hydroxyl thiophenol. After redispersed in ethanol, and treated by ultrasonic vibration and percolation, solutions for spin-coating purpose are produced.

By replacing part of cadmium acetate with manganese acetate, we prepared Mn doped CdS nanoparticles with different concentrations of manganese (5%, 10% and 20%, in molar%). Through out the experiment, no significant difference of doped and undoped CdS nanoparticles is found under the spectral resolution of our monochromator.

The second form of CdS nanoparticle is coated with silica shell. The purpose of preventive use of organic component is to raise the thermal budget of whole fabrication process. The preparation process is as follows. Cadmium acetate dihydrate ($\text{Cd}(\text{CH}_3\text{COO})_2 \cdot 2\text{H}_2\text{O}$, 1.60 g, 6.0 mmole) is dissolved in 32 ml mixed solvent of acetonitrile and water with volume ratio 1:1. Another solution containing disodium sulfide ($\text{Na}_2\text{S} \cdot x\text{H}_2\text{O}$, $x=7-9$, 0.58 g, ~2.4 mmole) and (γ -mercaptopropyl) trimethoxysilane (1.41 g, 7.2 mmole) in the same solvent system is added into vigorously stirred solution of cadmium acetate. After being vigorously stirred for 18 hours, the mixture is basified to pH=8.4 with 25% of NH_3 aqueous solution. Additional 64 ml of ethanol is added to the mixture. The mixture is stirred for 48 hours after adding 1.89 g of orthotetraethoxysilane (TEOS). Part of the solvent was removed and precipitation takes place in the mixture. The precipitate is centrifuged for three times and rinsed with deionized water. We obtained 2.30 g of light yellow powder after drying with vacuum. To fabricate LEDs, we dispersed 0.1 g of the powder into 10 ml of ethanol for spin-coating process. With ultrasonic vibration and percolation, solutions for spin-coating purpose are produced.

To take TEM image, prepared solution is dipped onto carbon film coated copper plate and reabsorbed. Sparsely distributed nanoparticles are obtained. The average diameter of the spherical CdS nanoparticles is about 5 nm, as shown in Fig. 1.

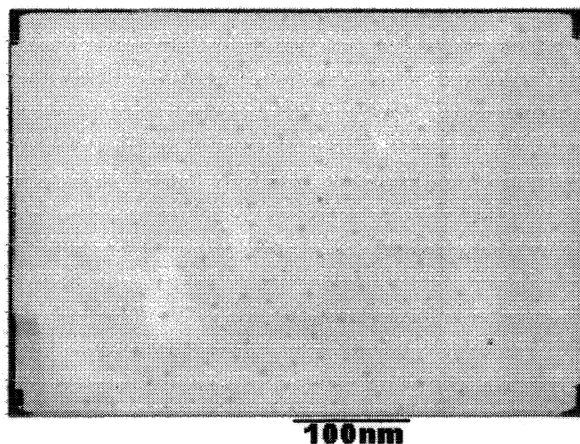


Fig. 1: TEM image of p-hydroxyl thiophenol capped CdS nanoparticles.

3. FABRICATION OF LED

The CdS light emitting diodes on silicon wafer are fabricated in different conditions. They are described in three parts according to the investigation of electroluminescence spectrum under those conditions. Although the primitive CdS nanoparticle EL could be found for all conditions, heat treatment and oxygen environment are discovered to have significant effects on the spectrum. Physical mechanisms for radiative recombination in these EL samples are different.

3.1 Normal process

A schematic of the CdS-nanoparticle LED is shown in Fig. 2. The fabrication steps are as follows. First, a fairly doped silicon wafer (doping $\sim 10^{15} \text{ cm}^{-3}$) is used as substrate. Acetone, methanol, and DI water are used successively for clean procedure. The wafer is placed on spinner with several dips of CdS nanoparticle solutions. A spin speed of 4000 rpm for 60 sec is used. For the EL investigation in this section, the wafer is placed in a chamber treated with vacuum at room temperature for 5 minutes to remove ethanol solvents. The thickness of CdS nanoparticle layer can be as large as 500 nm, verified by surface profile scan. As a result, volume density is very high, but relative high level of resistance also present, and could result in large voltage drop over the diode.

Subsequently, both top and bottom metal contacts are made by thermal evaporation. The top semi-transparent contact layer is 10nm gold, and the bottom is 150nm gold. Before the deposition of the Au layer, a 3-nm adhesion layer of chromium had been evaporated for both contacts. After voltage bias is applied, EL through top thin layer can be seen by naked eyes. A CM110 monochromator and photomultiplier is used to record the spectrum. In every spectrum measurement, the entrance slit width 0.6 mm is used for maximum detection and correct spectrum.

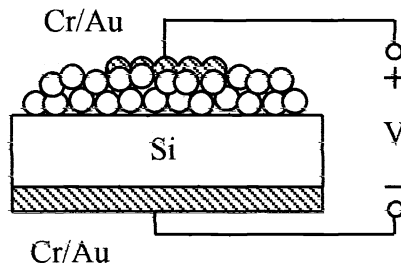


Fig.2: Schematic of the CdS nanoparticles EL device on Si wafer.

Samples made on n- and p-type Si wafers show different current-voltage curves, as shown in Fig. 3. Both have rectifying current-voltage (I-V) curves, but with opposite polarities. Those deposited on n-type silicon (solid line) exhibit large current when the nanoparticle side is positively biased and small current when the bias is reversed. Those

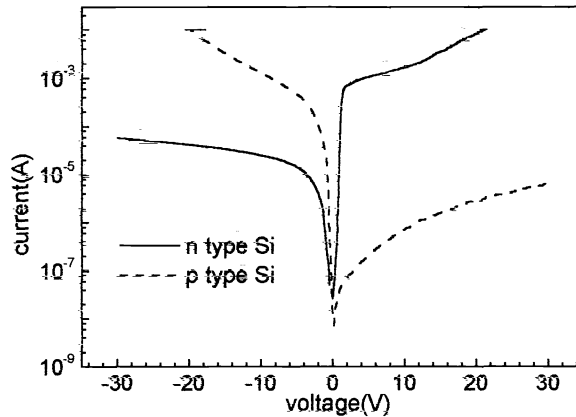


Fig.3: I-V curves of devices on n-type and p-type Si.

deposited on p-type silicon exhibit reverse behaviors. This rectifying effect corresponds to metal-insulator-semiconductor tunneling effect. To be specific, the thin potential barrier of organic coating and low substrate doping level result in Schottky-diode-like behavior. The EL spectrum corresponds to radiative recombination of carriers confined within CdS nanoparticles. Carriers are supplied by tunneling current.

For samples on the n-type substrate, schematically shown in Fig. 4, the Fermi level of Si has to be raised so that electrons are able to tunnel through the potential barrier of p-hydroxyl thiophenol group. Within CdS nanoparticles, part of the injected carriers recombine radiatively, part of them get trapped in defect levels, and part of them tunnel into the adjacent nanoparticles. Electrons trapped in oxygen-impurity level could also radiatively transit to valence band later on. Such process becomes significant if we immerse the nanoparticles into high concentration oxygen surrounding environment.

Both spectra of CdS and CdS doped with Mn are the same, as shown in Fig. 5. The spectrum fits into Lorentzian shape with scattering time of 6 fs and its FWHM is 42 nm. Such broad spectrum indicates the dispersion of particle size. The emission mechanism could be radiative recombination of free exciton in CdS nanoparticles or with red-shift effect due to p-hydroxyl thiophenol groups.

To be specific, the green spectrum peaks at 526.5nm (2.355eV), different from bulk CdS A-exciton transition energy, 2.441eV (508nm) at room temperature. The energy red-shift 86 meV does not come from quantum confinement within the nanoparticles, since such effect increases the exciton energy whenever the particle size decreases^{4,5}. It is the

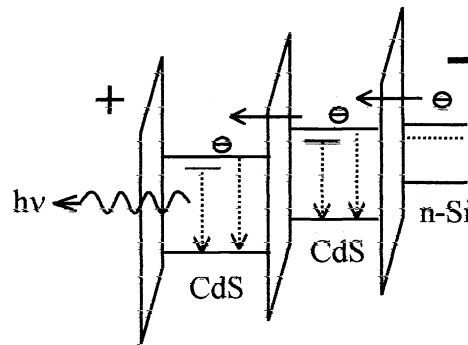


Fig. 4: Schematic of electron transport and transition in the device.

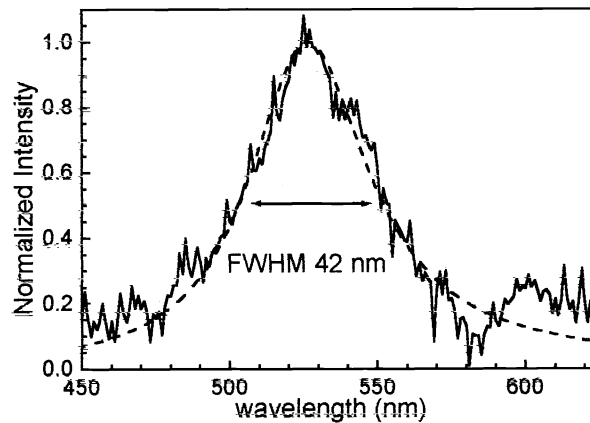


Fig. 5: EL Spectrum of CdS with direct vacuum treatment

capping p-hydroxyl thiophenol group that gives modification of the emission peak position. CdS nanoparticles coated with poly(vinyl alcohol) also show such energy shift in absorption spectrum⁶, where photoluminescence at 2.42eV (10K) is observed.

3.2. Heat treatment

The CdS nanoparticles are spin-coated as described in previous section. These samples are subsequently treated by rapid thermal annealing (RTA) with temperature 425°C for 5 minutes. The annealing process takes place in vacuum. No observable ash of the organic p-hydroxyl thiophenol group present, but the organic chemical is expected to decompose. I-V curves resemble that in Sec. 3.1. EL spectrum depicted in Fig. 6 shows two peaks. One is at 513.7nm and the other at 571.5nm. The former peak stands for bulk CdS signal (A exciton). This spectral lobe can be fitted by Lorentzian shape with scattering time of 8 fs and FWHM 40 nm.

The 571.5nm peak results from the trapped carriers in oxide-impurity levels⁷. High temperature environment and the decomposition of p-hydroxyl thiophenol group cause the diffusion process of oxygen into the nanoparticles to occur. This proves p-hydroxyl thiophenol group to be effective overcoat of CdS nanoparticles against oxygen. The oxide-

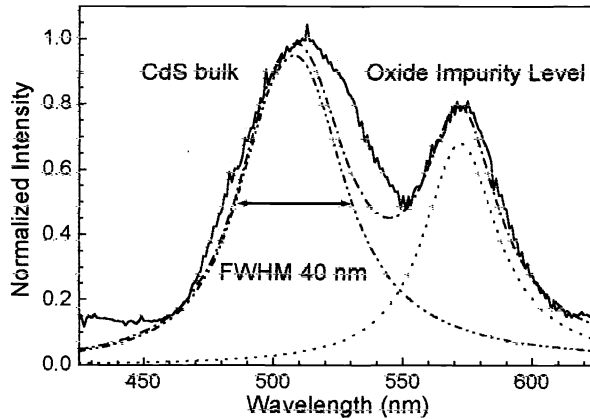


Fig. 6: The EL Spectrum of CdS particles after heat treatment.

impurity levels also induce radiative transition. The peak magnitude at the spectral lobe is smaller than the magnitude at 513.7nm, indicating that the emission from oxide-impurity levels is weaker than that resulted from the CdS nanoparticles. However, light power from this sample is stronger than that in Sec. 3.1. This phenomenon is ascribed as the participation of oxide-level luminescence, leading to enhancement of light emission.

3.3 Effect of surrounding oxides

To further study the oxide-impurity related signal, we immersed the CdS nanoparticles into high oxygen concentration environment. Two ways have proceeded. First, the nanoparticle solutions were mixed with SOG (spin-on-glass) 315FX, and the second way, mixed with SiO₂ nanoparticles (average diameter of 12 nm, dissolved in isopropanol). The cleaned, oxide-free silicon substrate is spin-coated and treated by 425°C RTA to sinter the SiO₂ glass. The similar EL spectrum is found in mixture of CdS nanoparticles with SOG and SiO₂ nanoparticles. The peak at 513.7nm (2.414eV) resembles A free exciton signal of bulk CdS at temperature 65°C, and the peak at 571.5nm (2.414eV) corresponds to radiative transition due to carriers trapped in oxide-impurity levels. The magnitude of total light emission in these samples is ten times stronger than that from unheated samples in Section 3.1, under the same carrier injection condition.

The spectra shown in and Fig.7 indicate two mechanisms. First, the coalescence of CdS nanoparticles into bulk form results in less broadening spectrum around 513.7 nm. Since the potential barrier of p-hydroxyl thiophenol group disappears due to decomposition, carriers in bulk powders stay for enough time (about 1ns transition lifetime) to recombine radiatively between each tunneling process. Second, relative magnitude of oxide-impurity-level luminescence is much stronger than that in Sec. 3.2. Highly increased concentration of oxide-impurity levels, which are supplied by surrounding oxides, contributes to the enhancement of internal quantum efficiency. The magnitude difference between mixture with SOG and SiO₂ nanoparticles comes from excess dangling Si-O bond of the latter case. With the same sintering time, the latter mixture makes oxygen diffusion easier. The energy diagram accounting for details of energy level is depicted in Fig.8. In bulk CdS, there are one conduction band and three split valence bands. Electron and hole recombine in free exciton form, with A, B, C notation. At room temperature, A free exciton peak of bulk CdS is 508nm, and at 65°C, it is 513.7nm. However the similar peak position does not lead to the conclusion that

origin of bulk CdS and CdS nanoparticles EL is the same. This becomes evident with EL behavior under varied temperature.

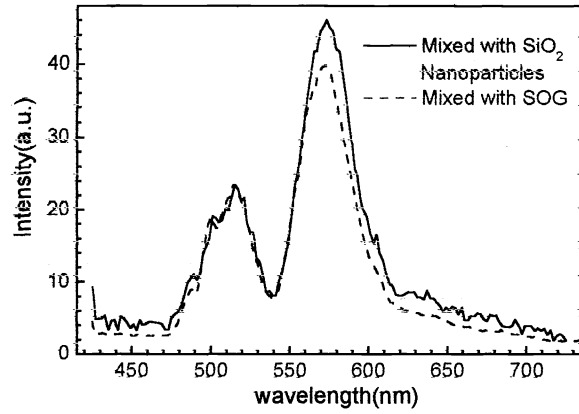


Fig. 7: EL spectrum of CdS nanoparticles with oxide-rich environment

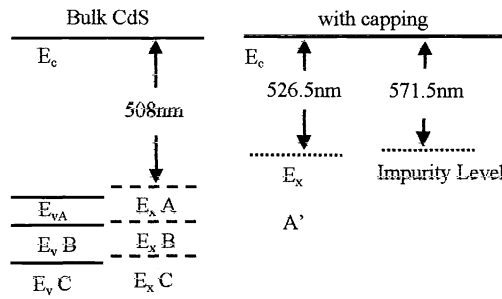


Fig. 8: Energy diagram showing different energy level involved.

3.4 Temperature effect

To examine EL property of CdS nanoparticle with varied temperature, original capping group is substituted with inorganic silica passivation shell, in order to prevent instability of organic composition at low temperature. The fabrication of LED is exactly the same as in Sec. 3.1. Familiar EL spectra of CdS nanoparticles silica-passivated samples are shown in Fig. 8. As temperature increases, the EL intensity decreases. Such reduced emission efficiency comes from increased nonradiative mechanisms with temperature. Surface trap states and carrier-phonon scattering both play roles. Ten times stronger magnitude of light emission intensity at low temperature of 15 K compared with room temperature case reveals that nonradiative mechanism is a crucial factor influencing emission efficiency of the emitter. The reason for the similar spectra is due to two causes. First, the shift of quantized energy levels due to small nanoparticles (<5nm) contributes to the spectrum around 520nm. Second, the oxide impurity level may have multiple levels corresponding to broad spectrum at room temperature.

Spectral peak at 520nm in Fig. 9 is attributed to the same origin as peak at 526.5nm in organic-capped CdS nanoparticles, with additional effect of quantum confinement and surface configuration. As a result, peak shift with varied temperature is compared with bulk bandgap shift in Fig. 10 and ascribed as characteristics of as-synthesized CdS nanoparticle. Ten times increase of emission intensity is observed at cryogenic temperature (15K), indicating strong influence of surface traps due to the large surface area. Reduced thermal scattering also contributes to enhancement of light emission at low temperature. The relative magnitude of oxide impurity level to exciton level changes slightly and may result from its nearness to conduction band

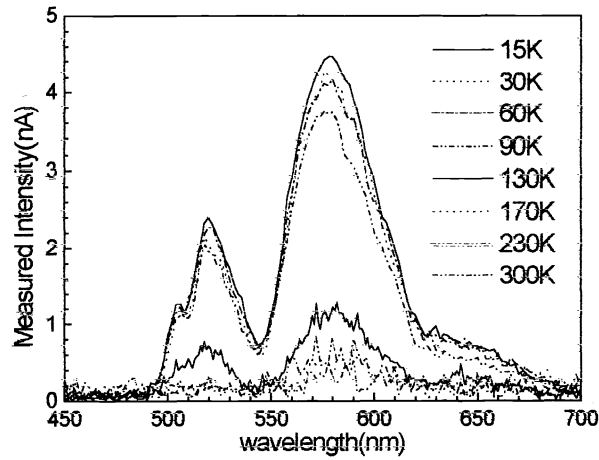


Fig. 9]: EL spectrum of CdS nanoparticles with silica shell at varied temperature.

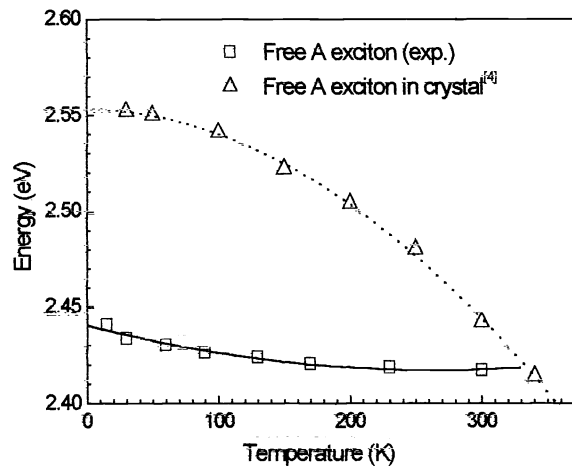


Fig. 10: Spectral peak variation with temperature compared with bulk exciton energy.

4. SPECTRUM ANALYSIS

The bulk CdS owns three valence bands, due to spin-orbit and crystal field splitting, and one conduction band. The electron in conduction band forms excitons with valence bands, ie. A,B,C exciton. Consider all three types of exciton A,B, and C, we have spontaneous light emission rate as

$$R_{sp}(\hbar\omega) = \sum_{i=A,B,C} G(\hbar\omega) \frac{\pi^2 \hbar^2 e^2}{\hbar\omega \epsilon m} \left| \langle u_c | p | u_v^{(i)} \rangle \right|^2 \times \sum_{(i)} \frac{1}{\omega^3} f_{ex} \delta(\hbar\omega - (E_g^{(i)} - E_B^{(i)})) \quad (1)$$

where photon density is

$$G(\hbar\omega) = \frac{\omega^2}{2\pi^2 \hbar^3 c^3}$$

exciton radius is $a_{ex} = \frac{e^2}{4\pi\epsilon E_B^{(i)}}$

and occupation probability approximated by Maxwell-Boltzman distribution is

$$f_{ex} = \exp(E_F - (E_g^{(i)} - E_B^{(i)} / n^2))$$

Here we assume all the three types of exciton A,B and C share the same Fermi level E_F . Collecting all terms and ignore constants at nearby energy 2.42eV (512nm) and consider only the most important $n=1$ peak, we obtain simplified relation.

$$R_{sp}(\hbar\omega) \propto \sum_{i=A,B,C} \left| \langle u_c | p | u_v^{(i)} \rangle \right|^2 \frac{\exp\left(\frac{-E_g^{(i)} + E_B^{(i)}}{kT}\right)}{(E_B^{(i)})^3} \times \delta(\hbar\omega - E_g^{(i)} + E_B^{(i)}) \quad (2)$$

In order to gain more physical insight into light emission in CdS nanoparticles, theoretical fitting to EL spectrum in Fig. 7 is made and shown in Fig. 11. Since the spontaneous emission spectrum of bulk CdS is of exciton origin, we use (2). The bound energies of A, B, and C exciton are 29.4 meV, 29.4 meV, and 26 meV, respectively, and the bulk bandgap energy 2.4423eV at 65°C is adopted⁷. The matrix element p_{cv}^2 is found to be 1:0.7:8.3. After delta function is substituted by Lorentzian, scattering time 18fs and FWHM 29 nm are obtained, indicating reduction of size dispersion and coalescence into bulk form.

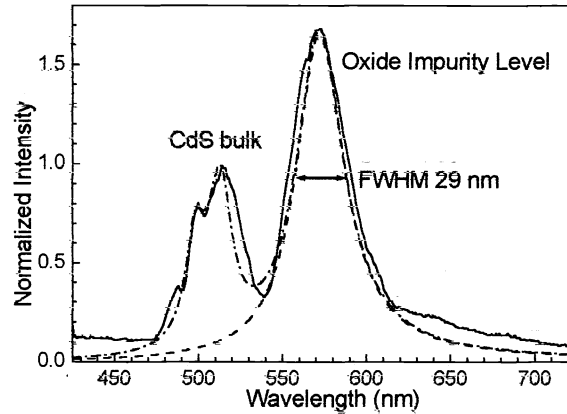


Fig. 11: Theoretical fitting of spectrum in Sec. 3.3.

With the energy parameters of bulk CdS given above, the energy shift due to p-hydroxyl thiophenol group in Section 3.1 is found to be 86 meV. Also, the oxide-impurity level is found to be 273 meV below the bandgap. In addition to current observation of such peak at 571.5nm, many other similar phenomena at the spectral range, 550nm~600nm, as an indication of imperfect CdS crystal or nanoparticles had also been found. Hong⁷ also demonstrated broad peak of 592nm (2.0944eV) due to S-vacancy (in this case substituting oxygen atom). Furthermore, Okamoto⁸ ascribed their broad peak at 650nm (1.9eV) to surface-trap-state emission, perhaps due to different process method. Previously observed transition of Mn^{2+} ion in CdS nanoparticle at 585nm (2.119eV)⁹ is not clearly observed in our samples, mainly due to insufficient spectral resolution.

5. CONCLUSIONS

Chemical preparation of CdS nanoparticles ready for spin-coating and LEDs made of CdS and CdS:Mn nanoparticles on Si substrates are described in detail. EL properties are investigated. Spectral shift of free exciton transition of 86 meV due to passivation of p-hydroxyl thiophenol group around nanoparticles is discovered. Process

modifications such as heat treatment and oxygen-rich environment are influential to intrinsic green emission. p-hydroxyl thiophenol group is shown to have protection from diffusion of contaminants into nanoparticles, but cannot resist temperature deterioration above 400°C.

Radiative recombination of carriers trapped in oxide-impurity levels of 273 meV below bandgap energy present. Ten times increase of emission intensity is observed at cryogenic temperature (15K), indicating strong influence of surface traps due to the large surface area. Reduced thermal scattering also contributes to enhancement of light emission at low temperature. At varied temperature, the EL spectrum of CdS nanoparticle remains quite the same. Peak shift is compared with bulk bandgap shift and ascribed as effect of quantum confinement and surface configuration.

ACKNOWLEDGEMENTS

The authors acknowledge the support from National Science Council, ROC under the contract NSC89-2112-M-002-076 and NSC89-2215-E-002-059.

REFERENCES

1. J. Butty, Y.Z. Hu, N. Peyghambarian, Y.H. Kao, and J.D. Mackenzie, "Quasicontinuous gain in sol-gel derived CdS quantum dots," *Appl. Phys. Lett.* **67**, pp.2672-2674, 1995.
2. V.I. Klimov, A.A. Mikhailovsky, Su Xu, A. Malko, J.A. Hollingsworth, C.A. Leatherdale, H.-J. Eisler, and M.G. Bawendi, "Optical Gain and Stimulated Emission in Nanocrystal Quantum Dots," *Science* **290**, pp.314-317, 2000.
3. J. G. C. Veinot, M. Ginzburg, and W. J. Pietro, "Surface Functionalization of Cadmium Sulfide Quantum-Confined Nanoclusters. 3. Formation and Derivatives of a Surface Phenolic Quantum Dot," *Chem. Mater.* **9**, pp.2117-2122, 1997.
4. B.G. Potter, Jr. and J.H. Simmons, "Quantum size effects in optical properties of CdS-glass composites," *Phys. Rev. B* **37**, pp.10838-10845, 1988.
5. M.V Rama Krishna, and R.A. Friesner, "Quantum confinement effects in semiconductor clusters," *J. Chem. Phys.* **95**, pp.8309-8322, 1991.
6. M. Tanaka, J. Qi, and Y. Masumoto, "Optical properties of undoped and Mn²⁺-doped CdS nanocrystals in polymer," *J. Crystal Growth* **214/215**, pp.410-414, 2000.
7. K.J. Hong, T.S. Jeong, C.J. Yoon, and Y.J. Shin, "The optical properties of CdS crystal grown by the sublimation method," *J. Crystal. Growth.* **218**, pp.19-26, 2000.
8. S. Okamoto, Y. Kanemitsu, H. Hosokawa, K. Murakoshi, and S. Yanagida, "Photoluminescence from surface-capped CdS nanocrystals by selective excitation," *Solid State Commun.* **105**, pp.7-11, 1998.
9. L. Spanhel, E. Arpac, and H. Schmidt, "Semiconductor clusters in the sol-gel process. Synthesis and properties of CdS nanocomposites," *J. Non. Cryst. Solids* **147/148**, pp.657-662, 1992.